Electronic Supplementary Material (ESI) for Inorganic Chemistry Frontiers.

Supplementary Information

Post-cyclotetramerization Strategy towards Novel Binuclear Phthalocyanine Dimers

Kang Wang,[†] Chunhua Huang,[†] Houhe Pan,[†] Nagao Kobayashi,[‡] and Jianzhuang Jiang[†,*]

Experimental Section

General. CH_2Cl_2 for voltammetric studies was distilled from CaH_2 under nitrogen. Column chromatography was carried out on silica gel (Merck, Kieselgel 60, 70-230 mesh) with the indicated eluents. **6**,[S1] **7**,[S1] and **8**[S1,S2] were prepared according to the published procedures. All other reagents and solvents were used as received.

^{1}H NMR spectra were recorded on a Bruker DPX 400 spectrometer. Spectrum was referenced internally using the resonances of $SiMe_4$ (δ = 0 for ^{1}H NMR). Electronic absorption spectra were recorded on a Hitachi U-4100 spectrophotometer. MCD spectra were recorded on a JASCO J-1500 CD Spectrometer with a JASCO electromagnet that produced a magnetic field of 1.60 T with both parallel and antiparallel fields. The magnitude of MCD features are expressed in terms of molar ellipticity ($[\theta]_M$ / deg M^{-1} cm^{-1} T^{-1}). IR spectra were recorded as KBr pellets using a Bruker Tensor 37 spectrometer with 2 cm^{-1} resolution. Elemental analyses were performed on an Elementar Vavio El III. MALDI-TOF mass spectra were taken on a Bruker BIFLEX III ultrahigh-resolution Fourier transformation cyclotron resonance (FT-ICR) mass spectrometer with alpha-cyano-4-hydroxycinnamic acid as matrix. The software of Bruker Daltonics IsotopePattern was used for the simulated mass pattern. Electrochemical measurements were carried out with a BAS CV-50W voltammetric analyzer. The cell comprised inlets for a glassy-carbon-disk working electrode of 2.0 mm in diameter and a silver-wire counter electrode. The reference electrode was Ag/Ag^+, which was connected to the solution by a Luggin capillary

whose tip was placed close to the working electrode. It was corrected for junction potentials by being referenced to the ferrocenium/ferrocene (Fe^{+}/Fe) couple ($E_{1/2}[Fe^{+}/Fe]$ = 501 mV vs SCE). Typically, a 0.1 M solution of $[Bu_4N][ClO_4]$ in CH_2Cl_2 containing 0.5 mmol dm^{-3} of sample was purged with nitrogen for 10 min. The voltammograms were then recorded at ambient temperature. The scan rate was 20 mV s^{-1} for differential pulse voltammetry. Crystal data for compound **3** was determined by X-ray diffraction analysis at 150 K using Oxford Diffraction Gemini E system with Cu Kα radiation λ = 1.5418 Å, and details of the structure refinement are given in Table S3. CCDC-1476231 containing the supplementary crystallographic data for this paper can be obtained free of charge from the Cambridge Crystallographic Data Centre *via* www.ccdc.cam.ac.uk/data_request/cif.

Synthesis of $H_2Pc(OR_1)_6$-$H_2Pc(OR_1)_6$ (1) in CH_2Cl_2 containing 0.1% TFA: Compound **6** (37.7 mg, 0.0310 mmol) was dissolved in 3.0 ml CH_2Cl_2 containing 0.1% TFA and stirred at room temperature for 5 h. Then, the reaction mixture was poured into water (10 mL) and extracted with CH_2Cl_2 (3 × 5 mL). The combined organic solution was then washed with water (3 × 10 mL) and dried with Na_2SO_4/K_2CO_3. After evaporating the solvent, the residue was chromatographed on a silica gel column using CH_2Cl_2 as the eluent. Repeated chromatography followed by recrystallization from $CHCl_3$ and CH_3OH gave **1** as green powder (4.4 mg, 12 %). ^1H NMR (400 MHz, $CDCl_3$) for **1**, δ: 9.32 (s, 4H), 8.33 (s, 4H), 8.09 (s, 4H), 7.38 (br, 36H), 2.58 (s, 24H), 2.47 (s, 24H), 2.36 (s, 24H), -0.23 ppm (s, 4H); MS (MALDI-

TOF): Calcd. for $C_{152}H_{124}N_{18}O_{12}$ $[M]^+$ 2393.6; found *m*/*z* 2393.9; Elemental analysis calcd (%) for $C_{152}H_{124}N_{18}O_{12}\cdot 2CHCl_3$: C 70.24, H 4.82, N 9.57; found: C 70.34, H 4.97, N 9.51.

Synthesis of $H_2Pc(OR_1)_6$-$H_2Pc(OR_1)_6$ (1) in pure CH_2Cl_2: By employing the above-mentioned procedure with pure CH_2Cl_2 instead of CH_2Cl_2 containing 0.1% TFA as solvent, only trace amount of **1** could be detected by MALDI-TOF spectrometry.

Synthesis of $H_2Pc(OR_1)_6$-$H_2Pc(OR_1)_6$ (1) in the mixed solvent of CH_2Cl_2 and TFA in the ratio of 99:1: By employing the above-mentioned procedure with the mixed solvent of CH_2Cl_2 and TFA in the ratio of 99:1 instead of CH_2Cl_2 containing 0.1% TFA, compound **1** was isolated in the yield of 20 %.

Synthesis of $H_2Pc(OR_1)_6$-$H_2Pc(OR_1)_6$ (1) in the mixed solvent of CH_2Cl_2 and TFA in the ratio of 95:5: By employing the above-mentioned procedure with the mixed solvent of CH_2Cl_2 and TFA in the ratio of 95:5 instead of CH_2Cl_2 containing 0.1% TFA, compound **1** was isolated in the yield of 44 %.

Synthesis of $H_2Pc(OR_1)_6$-$H_2Pc(OR_1)_6$ (1) in the mixed solvent of CH_2Cl_2 and TFA in the ratio of 90:10: By employing the above-mentioned procedure with the mixed solvent of CH_2Cl_2 and TFA in the ratio of 90:10 instead of CH_2Cl_2 containing 0.1% TFA, compound **1** was isolated in the yield of 50 %.

Synthesis of $H_2Pc(OR_1)_6$-$H_2Pc(OR_1)_6$ (1) in the mixed solvent of CH_2Cl_2 and TFA in the ratio of 80:20: By employing the above-mentioned procedure with the mixed solvent of CH_2Cl_2 and TFA in the ratio of 80:20 instead of CH_2Cl_2 containing 0.1% TFA, compound **1** was isolated in the yield of 72 %.

Synthesis of $H_2Pc(OR_1)_6$-$H_2Pc(OR_1)_6$ (1) in the mixed solvent of CH_2Cl_2 and TFA in the ratio of 70:30: By employing the above-mentioned procedure with the mixed solvent of CH_2Cl_2 and TFA in the ratio of 70:30 instead of CH_2Cl_2 containing 0.1% TFA, compound **1** was isolated in the yield of 59 %.

Synthesis of $H_2Pc(OR_1)_6$-$H_2Pc(OR_1)_6$ (1) in the mixed solvent of CH_2Cl_2 and TFA in the ratio of 60:40: By employing the above-mentioned procedure with the mixed solvent of CH_2Cl_2 and TFA in the ratio of 60:40 instead of CH_2Cl_2 containing 0.1% TFA, compound **1** was isolated in the yield of 55 %.

Synthesis of $H_2Pc(OR_1)_6$-$H_2Pc(OR_1)_6$ (1) in the mixed solvent of CH_2Cl_2 and TFA in the ratio of 40:60: By employing the above-mentioned procedure with the mixed solvent of CH_2Cl_2 and TFA in the ratio of 40:60 instead of CH_2Cl_2 containing 0.1% TFA, compound **1** was isolated in the yield of 47 %.

Synthesis of $H_2Pc(OR_1)_6$-$H_2Pc(OR_1)_6$ (1) in the mixed solvent of CH_2Cl_2 and TFA

in the ratio of 20:80: By employing the above-mentioned procedure with the mixed solvent of CH_2Cl_2 and TFA in the ratio of 20:80 instead of CH_2Cl_2 containing 0.1% TFA, compound **1** was isolated in the yield of 40 %.

Synthesis of $H_2Pc(OR_1)_6$-$H_2Pc(OR_1)_6$ (1) in pure TFA: By employing the above-mentioned procedure with pure TFA instead of CH_2Cl_2 containing 0.1% TFA as solvent, compound **1** was isolated in the yield of 21 %.

Synthesis of $ZnPc(OR_1)_6$-$ZnPc(OR_1)_6$ (3) in the mixed solvent of CH_2Cl_2 and TFA in the ratio of 80:20: By employing the above-mentioned procedure with compound **7** instead of compound **6** in the mixed solvent of CH_2Cl_2 and TFA in the ratio of 80:20, compound **3** was isolated in the yield of 56 %. ^{1}H NMR (400 MHz, $CDCl_3$-[D_5]pyridine (100:1)) for **3**, δ: 9.15 (s, 4H), 8.18 (s, 4H), 8.16, (s, 4H), 7.36 (br, 36H), 2.57 (s, 24H), 2.45 (s, 24H), 2.34 ppm (s, 24H); MS (MALDI-TOF): Calcd. for $Zn_2C_{152}H_{120}N_{18}O_{12}$ $[M]^+$ 2520.8; found *m*/*z* 2520.4; Elemental analysis calcd (%) for $Zn_2C_{152}H_{124}N_{18}O_{12}$: C 72.29, H 4.95, N 9.98; found: C 72.27, H 4.86, N 9.76.

Synthesis of $ZnPc(OR_1)_6$-$H_2Pc(OR_1)_6$ (2) in the mixed solvent of CH_2Cl_2 and TFA in the ratio of 80:20: The compounds **6** (28.3 mg, 0.0233 mmol) and **7** (29.8 mg, 0.0233 mmol) were dissolved in 3.0 ml mixed solvent of CH_2Cl_2 and TFA in the ratio of 80:20 and stirred at room temperature for 5 h. Then, the reaction mixture was poured into water (10 mL) and extracted with CH_2Cl_2 (3 × 5 mL). The combined

organic solution was then washed with water (3 × 10 mL) and dried with Na_2SO_4/K_2CO_3. After evaporating the solvent, the residue was chromatographed on a silica gel column using CH_2Cl_2 as the eluent to give a green band containing compound **1**, then using CH_2Cl_2/CH_3OH (100:1) as the eluent to give another green band containing compound **2** followed by a blue-green band containing compound **3**. Repeated chromatography followed by recrystallization from CH_2Cl_2 and CH_3OH gave **1** as green powder (5.8 mg, 10%), **2** as green powder (23.8 mg, 41%), and **3** as blue-green powder (4.7 mg, 8%), respectively. ^{1}H NMR (400 MHz, $CDCl_3$-[D_5]pyridine (100:1)) for **2**, δ = 9.28 (s, 2H), 9.22 (s, 2H), 8.34 (s, 2H), 8.18 (s, 2H), 8.16 (s, 2H), 8.10 (s, 2H), 7.36 (br, 36H), 2.58-2.59 (m, 24H), 2.46-2.47 (m, 24H), 2.38 (s, 12H), 2.34 (s, 12H), -0.26 ppm (s, 2H); MS (MALDI-TOF): Calcd. for $ZnC_{152}H_{122}N_{18}O_{12}$ $[M]^+$ 2456.9; found *m*/*z* 2456.8; Elemental analysis calcd (%) for $ZnC_{152}H_{122}N_{18}O_{12}$: C 74.27, H 5.00, N 10.26; found: C 74.34, H 4.97, N 10.51.

Synthesis of $H_2Pc(SR_2)_6$-$H_2Pc(SR_2)_6$ (4) and $H_2Pc(OR_1)_6$-$H_2Pc(SR_2)_6$ (5) in the mixed solvent of CH_2Cl_2 and TFA in the ratio of 80:20: The compounds **6** (28.3 mg, 0.0233 mmol) and **8** (23.3 mg, 0.0233 mmol) were dissolved in 3.0 ml mixed solvent of CH_2Cl_2 and TFA in the ratio of 80:20 and stirred at room temperature for 5 h. Then, the reaction mixture was poured into water (10 mL) and extracted with CH_2Cl_2 (3 × 5 mL). The combined organic solution was then washed with water (3 × 10 mL) and dried with Na_2SO_4/K_2CO_3. After evaporating the solvent, the residue was chromatographed on a silica gel column using CH_2Cl_2/*n*-hexane (2:1) as the eluent to

give a green band containing compound **5** followed by a brown band containing compound **4**. Then using CH_2Cl_2 as the eluent gave another green band containing compound **1**. Repeated chromatography followed by recrystallization from CH_2Cl_2 and CH_3OH gave **1** as green powder (15.5 mg, 30%), **4** as brown powder (11.1 mg, 21%), and **5** as green powder (3.8 mg, 7.4%), respectively. MS (MALDI-TOF) for **4**: Calcd. for $C_{128}H_{172}N_{18}S_{12}$ $[M]^+$ 2348.1; found *m*/*z* 2447.4; Elemental analysis calcd (%) for $C_{128}H_{172}N_{18}S_{12}\cdot 4CH_2Cl_2$: C 58.99, H 6.75, N 9.38; found: C 58.72, H 6.82, N 9.65. ^{1}H NMR (400 MHz, $CDCl_3$) for **5**, δ = 9.96 (s, 2H), 9.10 (s, 2H), 8.44 (s, 2H), 8.12 (s, 2H), 8.10 (s, 2H), 7.72 (m, 4H), 7.58 (m, 4H), 7.53 (m, 2H), 7.42 (m, 8H), 6.99 (s, 2H), 4.23 (m, 6H), 4.06 (m, 2H), 3.63 (br, 12H), 3.44 (br, 8H), 3.13 (br, 8H), 2.60 (s, 12H), 2.52 (m, 12H), 2.49 (s, 12H), 1.98 (br, 12H), 1.42 (br, 30H), -0.24 ppm (s, 4H); MS (MALDI-TOF): Calcd. for $C_{140}H_{148}N_{18}O_6S_6$ $[M]^+$ 2370.1; found *m*/*z* 2370.5. Elemental analysis calcd (%) for $C_{140}H_{148}N_{18}O_6S_6\cdot 5CH_2Cl_2$: C 62.29, H 5.70, N 9.01; found: C 61.93, H 5.63, N 9.10.

Spectroscopic characterization. Satisfactory ^{1}H NMR spectrum was obtained for $H_2Pc(OR_1)_6$-$H_2Pc(OR_1)_6$ (**1**) in $CDCl_3$, Fig. S2 and Table S1. As can be seen, the singlet signals appearing at δ = 9.32, 8.33, and 8.09 ppm in the spectrum of **1** can be assigned to the Pc α-protons. The broad peak at δ = 7.38 ppm is attributed to the aromatic protons of the substituents, while the three singlets at δ = 2.58, 2.47, and 2.36 ppm are due to the methyl protons. The singlet signal appearing at δ = -0.23 was assigned to the inner protons of the metal free homobinuclear phthalocyanine dimer. The ^{1}H NMR spectra of $ZnPc(OR_1)_6$-$H_2Pc(OR_1)_6$ (**2**) and $ZnPc(OR_1)_6$-$ZnPc(OR_1)_6$ (**3**) displayed broad and indistinguishable signals in pure $CDCl_3$ due to some extent of aggregation. Fortunately, this problem could be resolved by using a mixed solvent of $CDCl_3$-[D_5]pyridine (100:1). The ^{1}H NMR spectrum of **3** can be assigned in a similar manner as for **1** except for the disappearance of the inner proton signal, Fig. S3 and Table S1. Owing to the reduced symmetry, the ^{1}H NMR spectrum of the heterobinuclear dimer $ZnPc(OR_1)_6$-$H_2Pc(OR_1)_6$ (**2**) exhibits six Pc α-proton singlets at δ = 9.28, 9.22, 8.34, 8.18, 8.16, and 8.10 ppm, one broad peak at δ = 7.36 ppm attributed to the aromatic protons of the substituents, two multiplet signals at 2.58-2.59 and 2.46-2.47 ppm and two singlets at 2.38 and 2.34 ppm due to the methyl protons, and one inner proton singlet at -0.26 ppm, Fig. S4 and Table S1. The other heterobinuclear phthalocyanine dimer $H_2Pc(OR_1)_6$-$H_2Pc(SR_2)_6$ (**5**) exhibits six Pc α-proton singlets at δ = 9.96, 9.10, 8.44, 8.12, 8.10, and 6.99 ppm, four multiplets at δ = 7.72, 7.58, 7.53, and 7.42 ppm due to the aromatic protons of the 2,6-dimethylphenoxy substituents, two multiplet signals at 4.23 and 4.06 ppm and five

broad peaks at 3.63, 3.44, 3.13, 1.98, and 1.42 ppm due to the protons of the hexylthio group, and three singlets at 2.60, 2.52, and 2.49 ppm due to the methyl protons of the 2,6-dimethylphenoxy substituents, and one inner proton singlet at -0.24 ppm, Fig. S5 and Table S1.

Figs. S7-S11 exhibit the IR spectra of **1**-**5**. In the IR spectra, in addition to the absorption bands contributed from the central aromatic Pc macrocycle including the wagging and torsion vibrations of C-H groups, isoindole ring stretching vibrations, and the C=N aza group stretching vibrations,[S3] the newly observed absorptions around 2848, 2920, and 2951 cm^{-1} due to the antisymmetric C-H stretching vibrations of the 2,6-dimethylphenoxy/hexylthio groups.[S4,S5] In addition, in the IR spectra of **1**, **2**, **4**, and **5**, weak bands at *ca.* 3300 cm^{-1} can be assigned to the asymmetrical N-H stretching vibration of the isoindole moieties,[S3] which disappears in the IR spectrum of **3**.

Electrochemical Properties. The electrochemical properties of **1**-**3** and **5** were studied by differential pulse voltammetry (DPV) in CH_2Cl_2. However, due to the intensive aggregation behavior under the present experimental condition, the DPV of **5** could not give any meaningful information. As a consequence, only the half-wave redox potentials of compounds **1**-**3** are tabulated in Table S4. Fig. S12 shows the DPV of **1** as a typical representative. According to the DPV results, **1**-**3** display two quasi-reversible one-electron oxidations (labeled as Oxd_1 and Oxd_2) and four quasi-reversible one-electron reductions (Red_1-Red_4) within the electrochemical window of

CH_2Cl_2. All the processes for **1-3** are attributed to successive removal from or addition of one electron to the ligand-based orbitals. As shown in Table S4, in comparison with the metal free phthalocyanine dimer **1**, all the oxidation and reduction potentials for **2** take cathodic shift due to the replacement of 2H in **1** by one zinc ion in **2**. Further cathodic shift was observed in corresponding redox potentials for **3** relative to **2** following the replacement of the remaining 2H in **2** by Zn in **3**. However, the potential difference between Oxd_1 and Red_1 ($\Delta E^o_{1/2}$) for these three compounds keeps almost unchanged, in line with the observation of their Q band absorption in the similar region.

References

S1 (a) D. Wöhrle, M. Eskes, K. Shigehara and A. Yamada, *Synthesis*, 1993, 194 - 196; (b) H. Pan, C. Chen, K. Wang, W. Li and J. Jiang, *Chem. Eur. J.*, 2015, **21**, 3168-3173; (c) T. Ikeue, T. Fukahori, T. Mitsumune, K. Ueda, K. Fujii, S. Kurahashi, M. Koikawa, T. Sugimori, I. Hiromitsu, K. Yoshino, M. Mikuriya and M. Handa, *Inorg. Chim. Acta*, 2014, **409**, 433–440.

S2 Y. Zhang, P. Ma, P. Zhu, X. Zhang, Y. Gao, D. Qi, Y. Bian, N. Kobayashi and J. Jiang, *J. Mater. Chem.*, 2011, **21**, 6515-6524.

S3 (a) J. Jiang, M. Bao, L. Rintoul and D. P. Arnold, *Coord. Chem. Rev.*, 2006, **250**, 424-448; (b) S. Dong, D. Qi, Y. Zhang, J. Jiang and Y. Bian, *Vib. Spectrosc.*, 2011, **56**, 245-249.

S4 (a) H. Shang, H. Wang, W. Li and J. Jiang, *Vib. Spectrosc.*, 2013, **69**, 8–12;

(b) Y. Zhang, W. Cao, K. Wang and J. Jiang, *Dalton Trans.*, 2014, **43**, 9152-9157.

S5 (a) X. Zhang, Y. Zhang and J. Jiang, *Vib. Spectrosc.*, 2003, **33**, 153-161; (b) Y. Zhang, P. Ma, P. Zhu, X. Zhang, Y. Gao, D. Qi, Y. Bian, N. Kobayashi and J. Jiang, *J. Mater. Chem.*, 2011, **21**, 6515-6524.

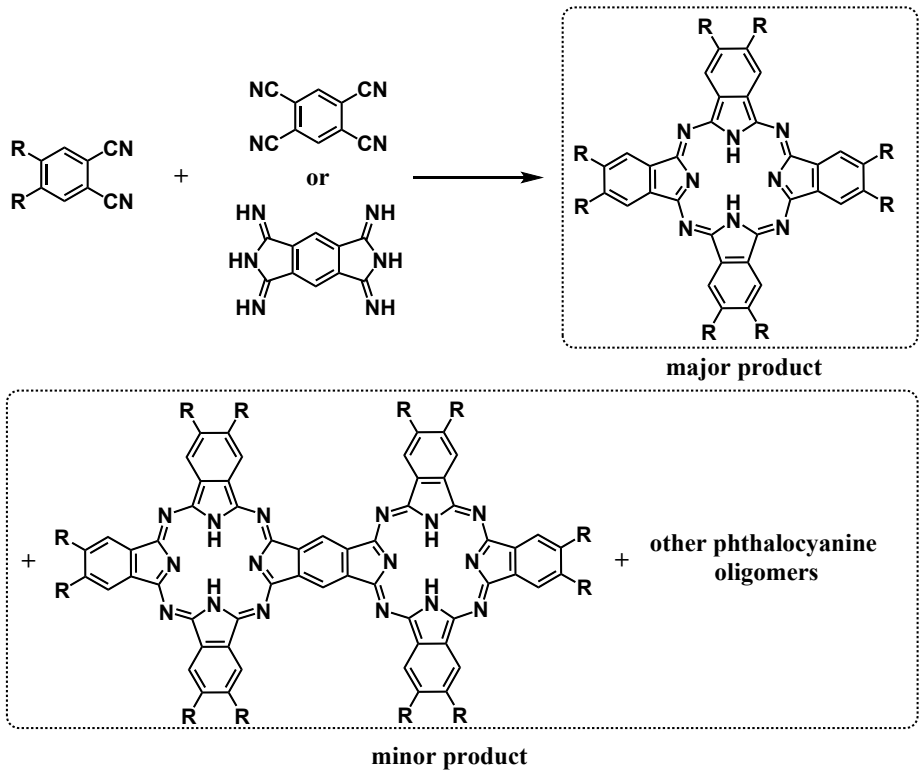

Scheme S1. Synthesis of π-conjugated phthalocyanine oligomers *through* the cyclotetramerization pathway with 1,2,4,5-tetracyanobenzene or its bis(diiminoisoindole) counterpart as the necessary precursor.

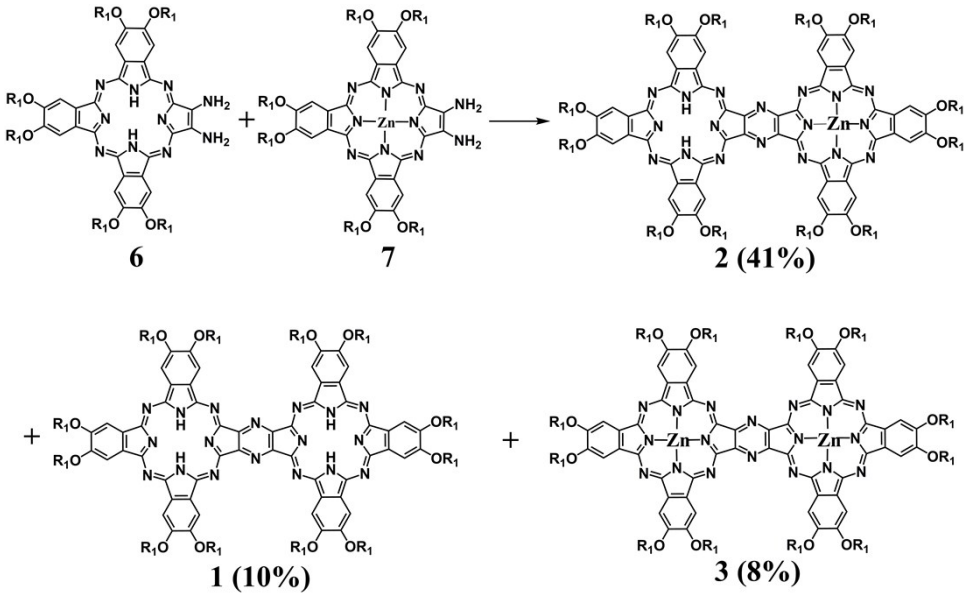

Scheme S2. Reaction between diamino-Pcs **6** and **7** in CH_2Cl_2/TFA (80:20) at the room temperature (OR_1 = 2,6-dimethylphenoxy).

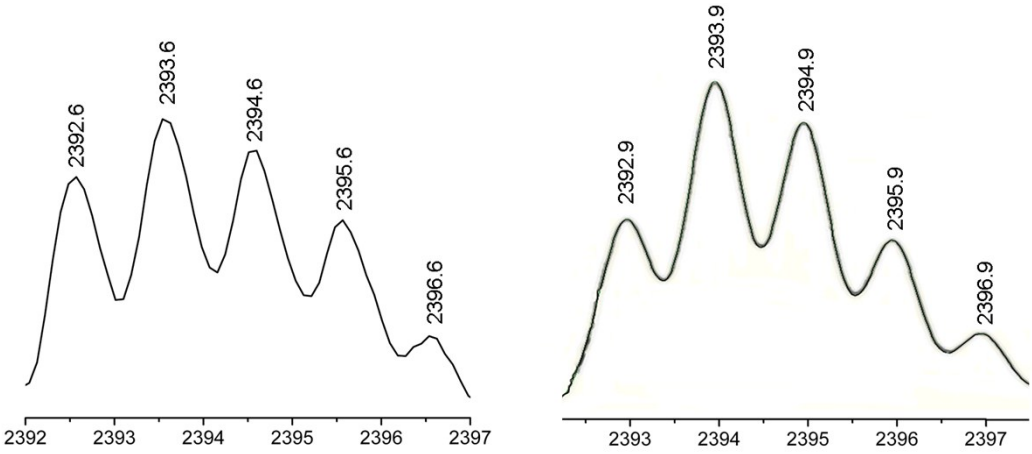

Fig. S1. Experimental (left) and simulated isotopic (right) pattern for the molecular ion of **1** shown in the MALDI-TOF mass spectrum.

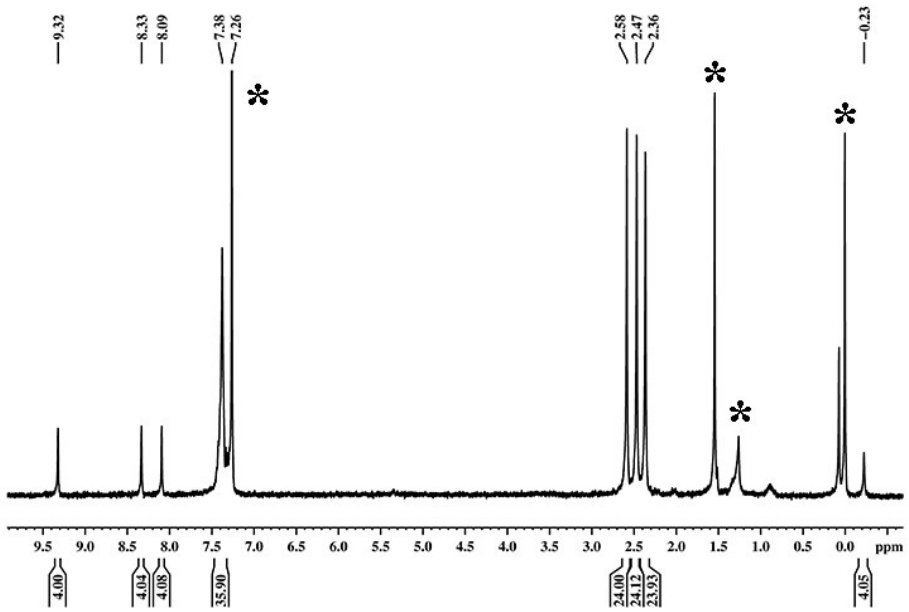

Fig. S2. ^{1}H NMR spectrum of compound **1** recorded in $CDCl_3$. *denotes the solvent impurity and the internal $SiMe_4$.

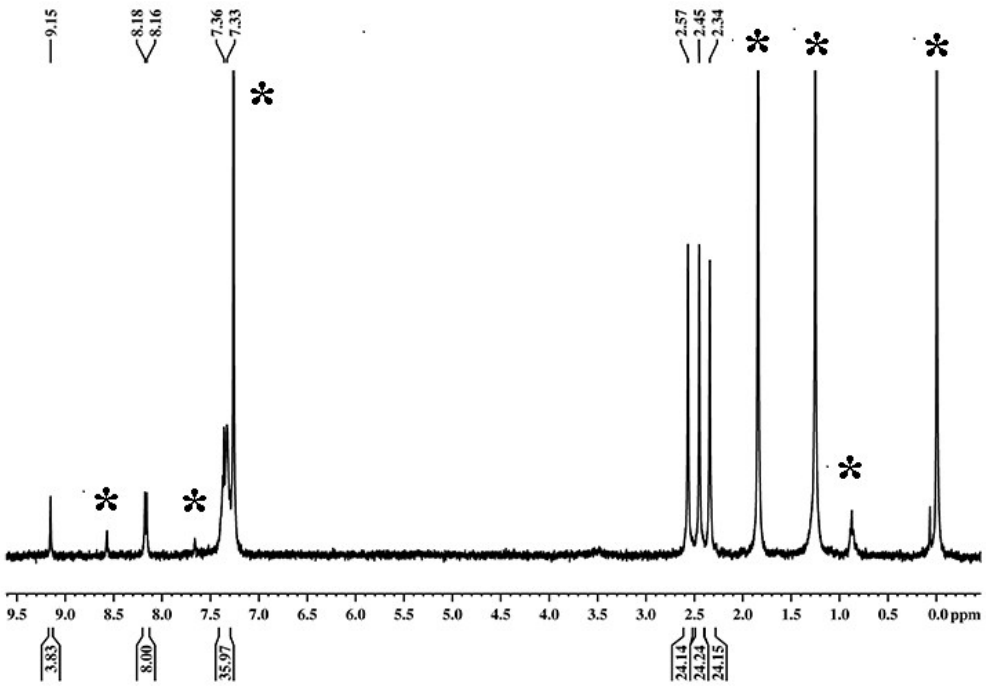

Fig. S3. ^{1}H NMR spectrum of compound **3** recorded in $CDCl_3$-[D_5]pyridine (100:1).

*denotes the solvent impurity and the internal $SiMe_4$.

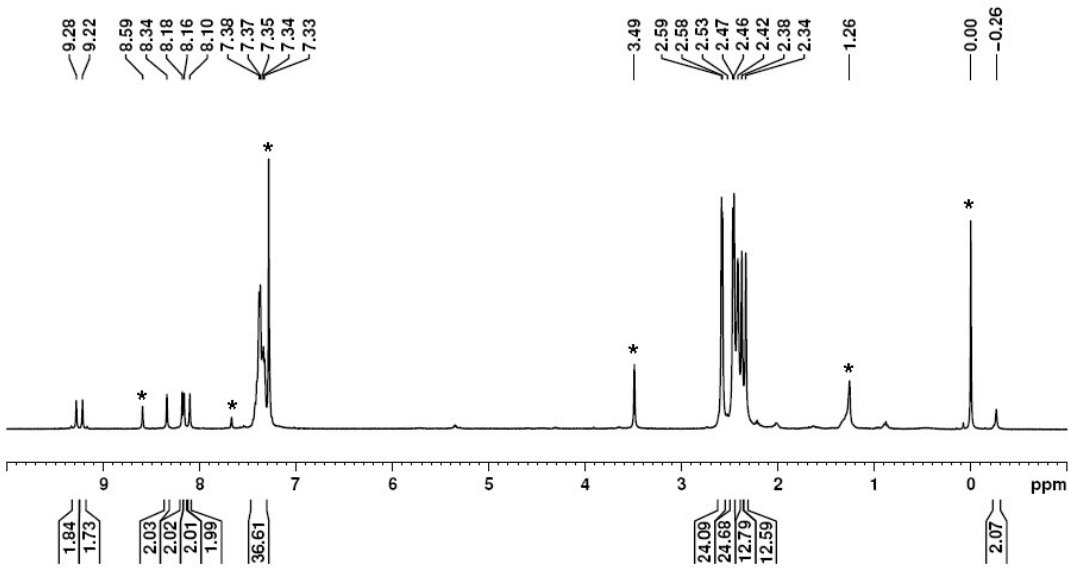

Fig. S4. ^{1}H NMR spectrum of compound **2** recorded in $CDCl_3$-[D_5]pyridine (100:1).

*denotes the solvent impurity and the internal $SiMe_4$.

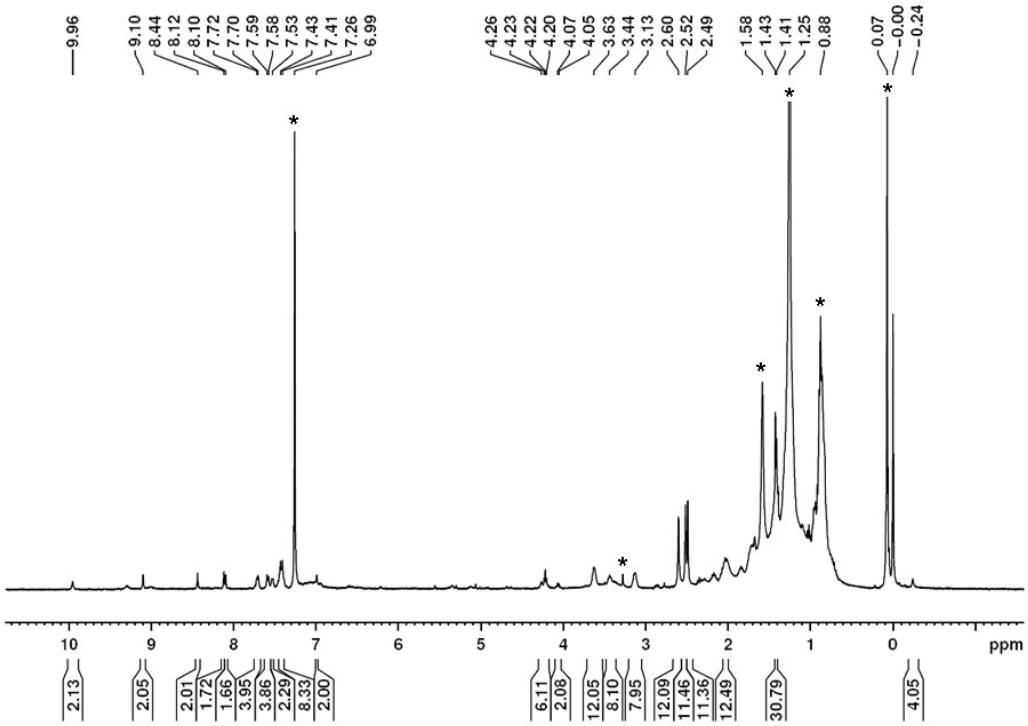

Fig. S5. ^{1}H NMR spectrum of compound **5** recorded in $CDCl_3$. *****denotes the solvent impurity and the internal $SiMe_4$.

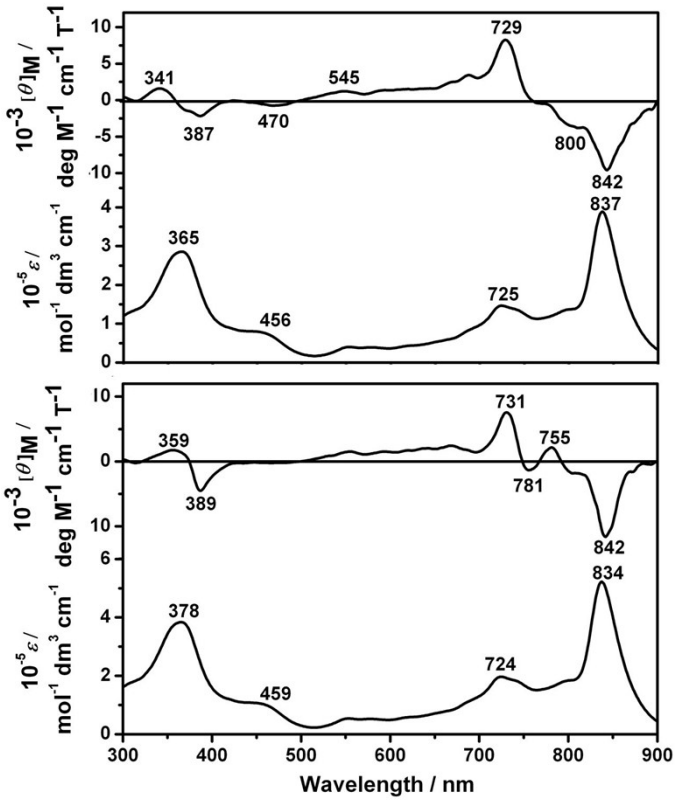

Fig. S6. Electronic absorption and MCD spectra of **2** (top) and **3** (bottom) in $CHCl_3$-pyridine (100:1).

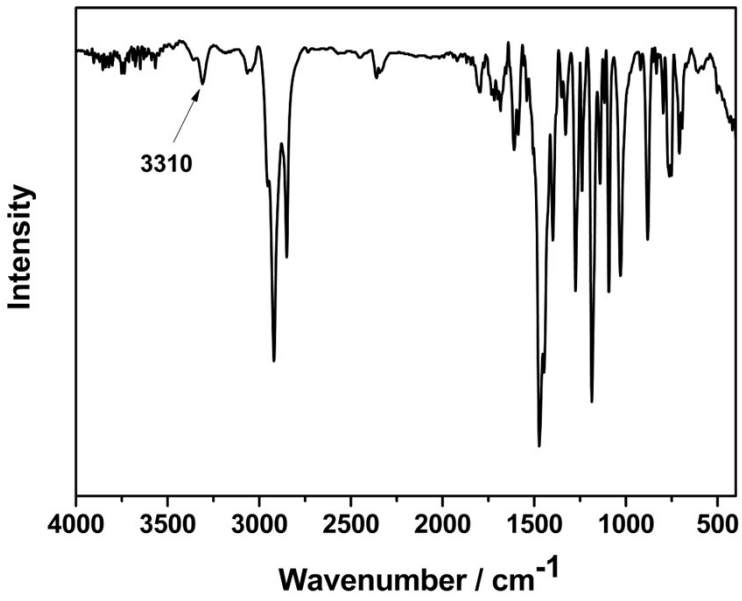

Fig. S7. The IR spectrum of **1** in the region of 400-4000 cm^{-1} with 2 cm^{-1} resolution.

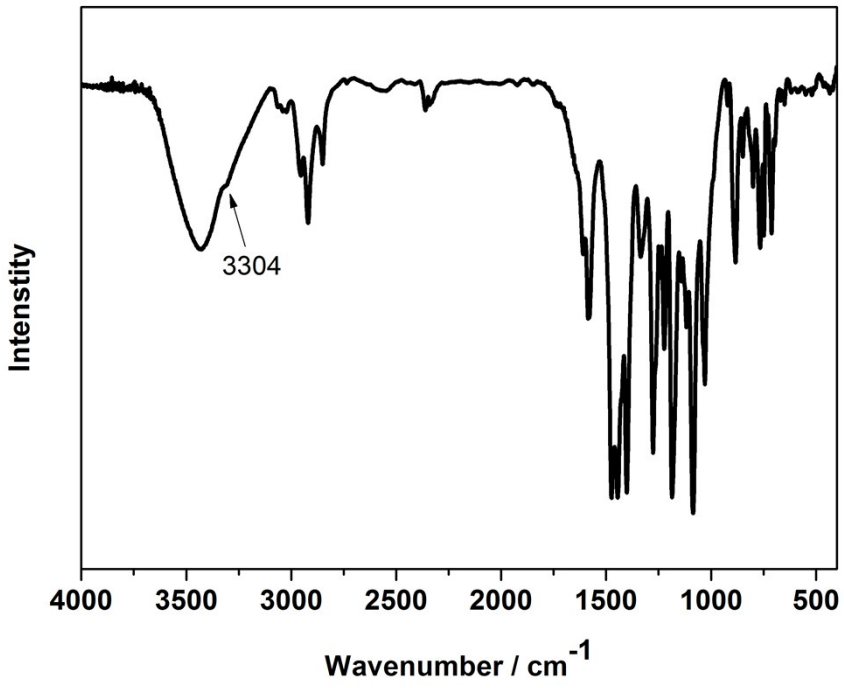

Fig. S8. The IR spectrum of **2** in the region of 400-4000 cm^{-1} with 2 cm^{-1} resolution.

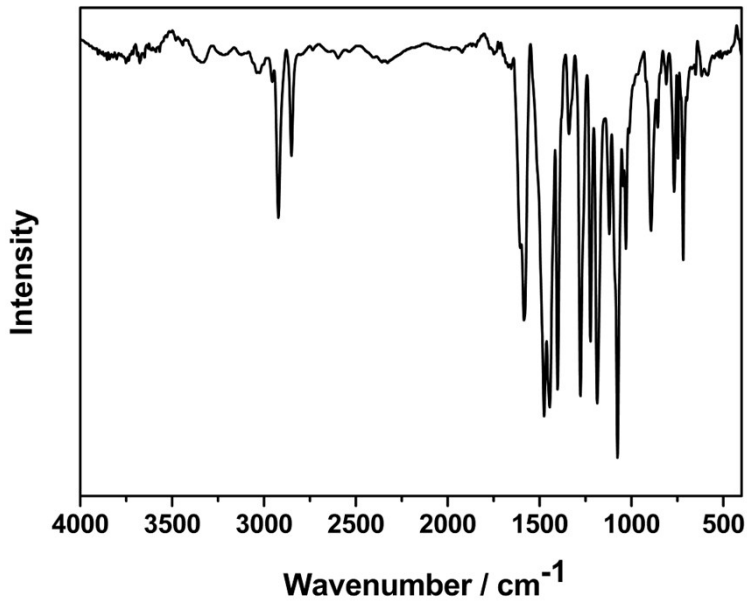

Fig. S9. The IR spectrum of **3** in the region of 400-4000 cm^{-1} with 2 cm^{-1} resolution.

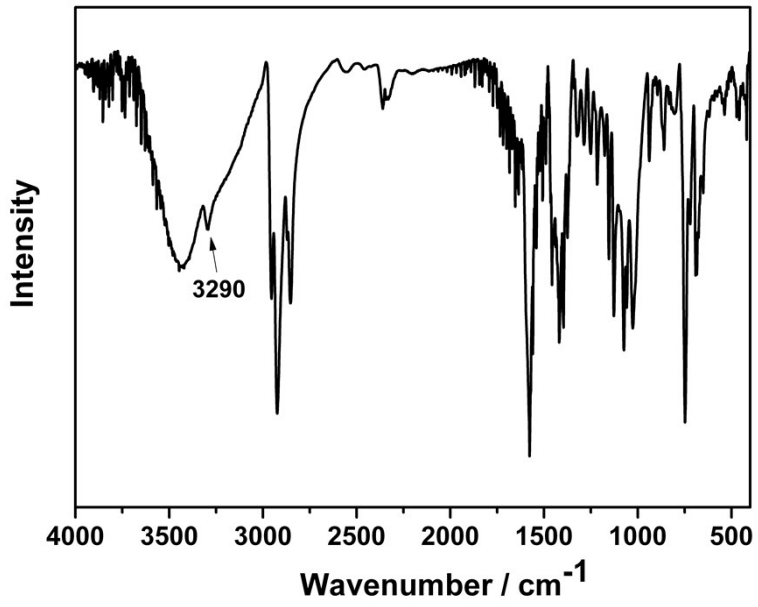

Fig. S10. The IR spectrum of **4** in the region of 400-4000 cm^{-1} with 2 cm^{-1} resolution.

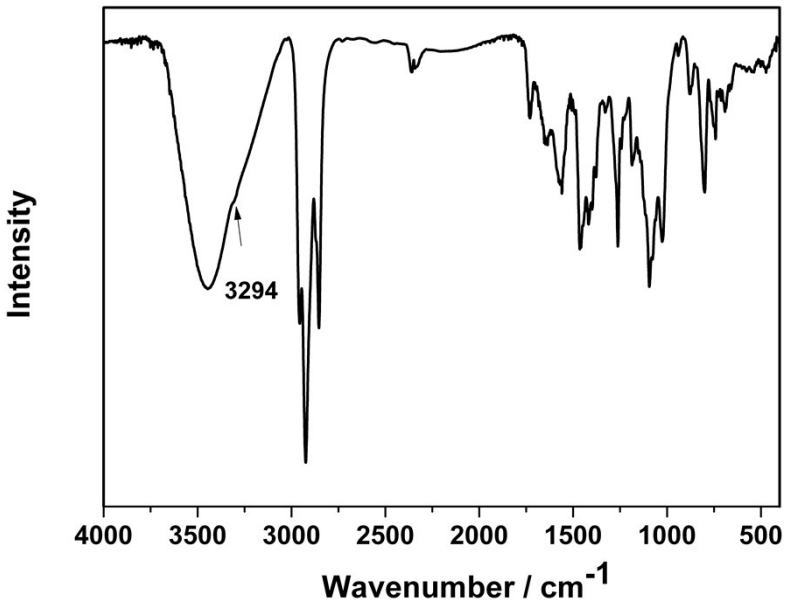

Fig. S11. The IR spectrum of **5** in the region of 400-4000 cm^{-1} with 2 cm^{-1} resolution.

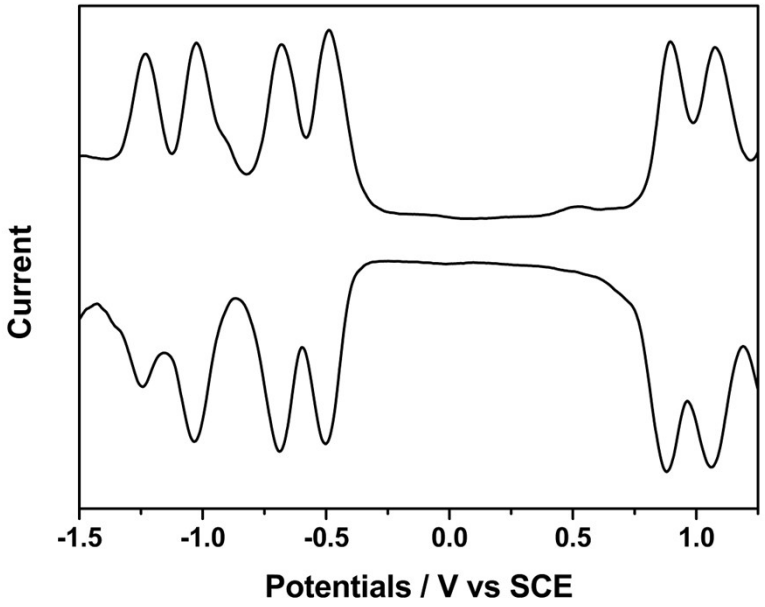

Fig. S12. Differential pulse voltammetry of **1** in CH_2Cl_2 containing 0.1 M $[NBu_4][ClO_4]$.

Table S1. ^{1}H NMR data (δ) and assignments of **1** and **5** in $CDCl_3$ as well as **2** and **3** in $CDCl_3$-[D_5]pyridine (100:1).

Compound	**H**$^{\alpha}$	Ph-**H**	**-CH$_3$**	-S**C$_6$H$_{13}$**	Inner-H
1	9.32 (s, 4H)	7.38 (br, 36H)	2.58 (s, 24H)	---	-0.23 (s, 4H)
	8.33 (s, 4H)		2.47 (s, 24H)		
	8.09 (s, 4H)		2.36 (s, 24H)		
2	9.28 (s, 2H)	7.36 (br, 36H)	2.58-2.59 (m, 24H)	---	-0.26 (s, 2H)
	9.22 (s, 2H)		2.46-2.47 (m, 24H)		
	8.34 (s, 2H)		2.38 (s, 12H)		
	8.18 (s, 2H)		2.34 (s, 12H)		
	8.16 (s, 2H)				
	8.10 (s, 2H)				
3	9.15 (s, 4H)	7.36 (br, 36H)	2.57 (s, 24H)	---	---
	8.18 (s, 4H)		2.45 (s, 24H)		
	8.16 (s, 4H)		2.34 (s, 24H)		
5	9.96 (s, 2H)			4.23 (m, 6H)	-0.24 (s, 4H)
	9.10 (s, 2H)	7.72 (m, 4H)		4.06 (m, 2H)	
	8.44 (s, 2H)	7.58 (m, 4H)	2.60 (s, 12H)	3.63 (br, 12H)	
	8.12 (s, 2H)	7.53 (m, 2H)	2.52 (s, 12H)	3.44 (br, 8H)	
	8.10 (s, 2H)	7.42 (m, 8H)	2.49 (s, 12H)	3.13 (br, 8H)	
	6.99 (s, 2H)			1.98 (br, 12H)	
				1.42 (br, 30H)	

Table S2. Electronic absorption spectroscopic data for compounds **1**-**3** and **5**.[a]

Compound	λ_{max} / nm (logε)				
1	356 (5.32)	455 (4.89)	719 (5.16)	740 (5.05)	830 (5.57)
2	365 (5.44)	456 (4.88)	551 (4.59)	725 (5.12)	837 (5.59)
3	378 (5.50)	553 (4.84)	724 (5.13)	743 (5.11)	834 (5.72)
5	346 (5.30)	----	723 (5.22)	---	837 (5.26)

[a]The electronic absorption spectrum of compounds **1** and **5** was recorded in $CHCl_3$, while those of the compounds **2** and **3** are recorded in $CHCl_3$-pyridine (100:1).

Table S3. Crystallographic data for compound **3**.

	compound **3**
formula	$C_{166}H_{122}Cl_{12}N_{20}O_{12}Zn_2$[a]
fw	3144.98
Crystal system	orthorhombic
Space group	*P* bca
a/Å	30.8754(9)
b/Å	15.5743(7)
c/Å	38.3804(14)
α/°	90.0
β/°	90.0
γ/°	90.0
U/Å^3	18456(1)
Z	4
D_c/g cm^{-3}	1.132
μ/mm^{-1}	2.375
Data collection range/°	3.0593 to 67.0037
F(000)	6472
R_1 [$I>2\sigma(I)$]	0.1244
wR_2 [$I>2\sigma(I)$]	0.3465
Goodness of fit	1.144
CCDC Number	1476231

[a]In this structure, the unit cells include a large region of disordered solvent molecules, which could not be modeled as discrete atomic sites. We employed PLATON/SQUEEZE to calculate the diffraction contribution of the solvent molecules and, thereby, to produce a set of solvent-free diffraction intensities. The SQUEEZE calculations showed a total solvent accessible area volume of 5097 Å^3 and the residual electron density amounted to 1667 electron per unit cell, corresponding to nearly 20 molecules of $CHCl_3$ and 28 molecules of CH_3OH (about 5 $CHCl_3$ and 7 CH_3OH molecules per asymmetric unit).

Table S4. Half-wave redox potentials *vs* SCE of compounds **1-3** in CH_2Cl_2 containing 0.1 M TBAP.

Compound	Oxd_2	Oxd_1	Red_1	Red_2	Red_3	Red_4	$\Delta E^o_{1/2}$[a]
1	+1.09	+0.91	-0.48	-0.67	-1.01	-1.22	1.39
2[a]	+0.95	+0.79	-0.54	-0.77	-1.11	-1.42	1.33
3[a]	+0.92	+0.68	-0.71	-0.91	-1.33	-1.54	1.39

[a] These compounds were measured in CH_2Cl_2/pyridine (v/v=100/1).